frontiers in
MICROBIOLOGY

ORIGINAL RESEARCH ARTICLE
published: 26 April 2012
doi: 10.3389/fmicb.2012.00150

The unique biogeochemical signature of the marine diazotroph *Trichodesmium*

Jochen Nuester[1]*, Stefan Vogt[2], Matthew Newville[3], Adam B. Kustka[4] and Benjamin S. Twining[1]

[1] *Bigelow Laboratory for Ocean Sciences, East Boothbay, ME, USA*
[2] *X-ray Science Division, Advanced Photon Source, Argonne National Laboratory, Argonne, IL, USA*
[3] *Center for Advanced Radiation Sources, The University of Chicago, Argonne, IL, USA*
[4] *Department of Earth and Environmental Sciences, Rutgers University, Newark, NJ, USA*

Edited by:
Martha Gledhill, University of Southampton, UK

Reviewed by:
Mark Moore, University of Southampton, UK
William Landing, Florida State University, USA

****Correspondence:***
Jochen Nuester, Bigelow Laboratory for Ocean Sciences, 60 Bigelow Drive, P.O. Box 380, East Boothbay, ME 04544, USA.
e-mail: jnuester@bigelow.org

The elemental composition of phytoplankton can depart from canonical Redfield values under conditions of nutrient limitation or production (e.g., N fixation). Similarly, the trace metal metallome of phytoplankton may be expected to vary as a function of both ambient nutrient concentrations and the biochemical processes of the cell. Diazotrophs such as the colonial cyanobacteria *Trichodesmium* are likely to have unique metal signatures due to their cell physiology. We present metal (Fe, V, Zn, Ni, Mo, Mn, Cu, Cd) quotas for *Trichodesmium* collected from the Sargasso Sea which highlight the unique metallome of this organism. The element concentrations of bulk colonies and trichomes sections were analyzed by ICP-MS and synchrotron x-ray fluorescence, respectively. The cells were characterized by low P contents but enrichment in V, Fe, Mo, Ni, and Zn in comparison to other phytoplankton. Vanadium was the most abundant metal in *Trichodesmium*, and the V quota was up to fourfold higher than the corresponding Fe quota. The stoichiometry of 600C:101N:1P (mol mol^{-1}) reflects P-limiting conditions. Iron and V were enriched in contiguous cells of 10 and 50% of *Trichodesmium* trichomes, respectively. The distribution of Ni differed from other elements, with the highest concentration in the transverse walls between attached cells. We hypothesize that the enrichments of V, Fe, Mo, and Ni are linked to the biochemical requirements for N fixation either directly through enrichment in the N-fixing enzyme nitrogenase or indirectly by the expression of enzymes responsible for the removal of reactive oxygen species. Unintentional uptake of V via P pathways may also be occurring. Overall, the cellular content of trace metals and macronutrients differs significantly from the (extended) Redfield ratio. The *Trichodesmium* metallome is an example of how physiology and environmental conditions can cause significant deviations from the idealized stoichiometry.

Keywords: extended redfield ratio, metallome, nitrogen fixation, vanadium, iron, nickel, zinc

INTRODUCTION

The biogeochemical cycling of many trace metals is controlled, to a large degree, by their incorporation into plankton biomass in surface waters and remineralization from degrading plankton at depth. This linkage was proposed for macronutrients by Redfield (Redfield, 1934, 1958; Redfield et al., 1963), and more recent studies have expanded the concept to metals (Morel and Hudson, 1985; Bruland et al., 1991; Ho et al., 2003). Indeed, the molar stoichiometry of particulate C:N:P in surface waters has been observed to be strikingly similar to stoichiometries of dissolved CO_2:nitrate:phosphate in deep ocean seawater (Sverdrup et al., 1942; Takahashi et al., 1985; Körtzinger et al., 2001). Similar relationships can be observed for trace metals, although the comparisons break down for metals with significant lithogenic inputs, redox transformations, or scavenging behavior (Morel, 2008). Despite the relative constancy of average C:N:P in the ocean, macronutrient ratios in specific ocean regions and specific phytoplankton groups depart significantly from the Redfield ratio (Sverdrup et al., 1942; Geider and La Roche, 2002; Arrigo, 2005). Similarly, although bulk plankton communities are often characterized by a fairly consistent metal stoichiometry (Bruland et al., 1991; Ho, 2006), individual species and taxonomic groups can vary significantly in their metal stoichiometries (or quotas), even when grown under the same conditions (Ho et al., 2003; Twining et al., 2004, 2011).

The elemental composition of phytoplankton can depart from canonical Redfield values under conditions of nutrient limitation or production (e.g., N fixation). The diazotrophic cyanobacterium *Trichodesmium* has significantly elevated N contents, relative to P, when fixing N (White et al., 2006), and blooms of *Trichodesmium* can significantly alter the major nutrient stoichiometry of particular matter in surface waters of the ocean (Karl et al., 1992). Phytoplankton also vary their major nutrient stoichiometry under P-limiting conditions (Sterner and Elser, 2002; Ji and Sherrell, 2008), which may be encountered by *Trichodesmium* in the ocean (Sañudo-Wilhelmy et al., 2001). Macronutrient limitation can also result in altered trace metal stoichiometries as cells adjust their biochemical machinery to deal with changing nutrient supplies. For

example, cells require more Fe, Ni, and Zn to grow on nitrate, urea, and organic P, respectively, because of the biochemical composition of the metalloenzymes nitrate reductase, urease, and alkaline phosphatase (Price and Morel, 1991; Maldonado and Price, 1996; Ji and Sherrell, 2008). Additionally, taxonomic groups can vary in their metal response to identical macronutrient stresses (Ji and Sherrell, 2008).

Similarly, diazotrophs such as *Trichodesmium* are likely to have unique metal signatures due to their cell physiology. The metalloenzyme nitrogenase contains at least 38 atoms of Fe per holozyme (Whittaker et al., 2011). Kustka et al. (2003b) estimated that 19–53% of cellular Fe in *Trichodesmium* is bound in nitrogenase. Such presence of Fe-rich enzymes leads consequently to elevated Fe quotas in comparison to other phytoplankton (Berman-Frank et al., 2001). Cellular Mo enrichment relative to non-diazotrophic phytoplankton also likely results from the presence of a Mo and Fe (MoFe) cofactor of nitrogenase (Dominic et al., 2000; Tuit et al., 2004). Furthermore, the concomitant fixation of N and C in *Trichodesmium* requires an additional biochemical defense mechanism against reactive oxygen species, which deactivate the nitrogenase enzyme. The removal of hydrogen peroxide or superoxide by enzymes such haloperoxidase and superoxide dismutase is thus essential for the process of N fixation (Dupont et al., 2008b; Johnson et al., 2011). These enzymes have metal co-factors of their own which may be elevated in *Trichodesmium*, thus imparting to the organism a unique trace metal stoichiometry.

In this study we present data on the metal contents, or metallome (Williams, 2001; Haraguchi, 2004), of *Trichodesmium* collected from the Sargasso Sea in the western sub-tropical North Atlantic Ocean. Metal stoichiometries of whole colonies were determined using inductively coupled plasma mass spectrometry (ICP-MS), and trichome sections were assayed using synchrotron x-ray fluorescence (SXRF). In addition to providing independent assessment of the elemental content of the organisms, the micro-analytical analyses allow us to study the spatial allocation of these elements and probe their sources. Information about the metallome is then linked to the biology of *Trichodesmium* and several hypotheses are presented regarding the potential biochemical associations of these trace metals in this organism.

MATERIALS AND METHODS

SAMPLE COLLECTION

Trichodesmium samples were collected from the Sargasso Sea in August 2010 during a cruise to the region aboard the R/V Atlantic Explorer (Bermuda Atlantic Time-Series Study cruise 261). Samples were collected at six different stations at different times of the day. All stations were within a 13 km radius and were located within the same mesoscale water mass as indicated by sea surface height anomaly (**Figure 1**). Thus the stations are interpreted to represent one geographical location. *Trichodesmium* colonies were collected at a depth of ca. 5 m using a 100-μm plankton net with a PVC frame. Immediately after collection, 15–20 colonies were transferred using acid-washed polystyrene inoculation loops from the cod end to Teflon vials filled with Milli-Q water (> 18 MΩ) for subsequent digestion and ICP-MS analysis. In order to normalize metal quotas to C and N, as well as to P (which is obtained via ICP-MS), 20–30 colonies were concurrently picked at each station for CHN analysis and placed into Teflon vials filled with filtered seawater. Subsequently, colonies for CHN analysis were filtered onto pre-combusted GF/F filters, wrapped in aluminum foil, and frozen until samples could be dried overnight at 60°C. Additional samples were transferred from the cod end to two 50-mL centrifuge tubes and amended immediately with cleaned glutaraldehyde to a final concentration of 0.5% for preparation of SXRF samples.

All shipboard handling was carried out using trace metal clean materials and tools under a laminar flow hood. The elemental composition of whole colonies was determined using ICP-MS and CHN analysis (**Table 1**). Element distributions and concentrations in individual trichome sections were assessed with SXRF. Specific efforts to disaggregate colonies during SXRF sample preparation were not made, but individual free (i.e., non-overlapping) trichomes were chosen for analysis to enable interpretation of the resulting 2D element maps. No effort was made to identify or remove any attached bacteria, eukaryotes, or mineral material associated with colonies prior to analysis.

BULK ELEMENT ANALYSIS

Trichodesmium colonies were digested in Teflon vials prior to ICP-MS analysis. Vials were first cleaned via an overnight soak in 2 M HCl followed by boiling in aqua regia for 4 h. Vials were then rinsed five times with Milli-Q and dried in a class-100 laminar flow hood. *Trichodesmium* samples were digested in 6 M Optima HNO_3 at 150°C for 4 h. This was repeated twice with dry-down in between. Following digestion, each sample was taken up in 0.6 M HCl (Optima Grade) and In-115 was added as internal standard. Elemental contents of samples were more than 40-fold above those of blank digest vials that were filled with Milli-Q water in the field and treated exactly as samples. Digest blank values were subtracted from samples.

Samples were analyzed by high-resolution inductively coupled mass spectrometry (HR-ICP-MS, FinniganMAT, Element 2) using an Apex PFA desolvator/nebulizer (Elemental Scientific, Omaha, NE). A freshwater plankton standard (BCR-414, Commission of the European Communities) was analyzed to check analyte recoveries. The elements Al, Mn, Fe, Cu, and Zn had recoveries of $100 \pm 5\%$, while recoveries of Cd (110%), Mo (132%), and Ni (150%) were higher. *Trichodesmium* C and N quotas were determined using a Perkin-Elmer 2400 CHN analyzer. Element signals were 23- to 41-fold above those in blank ashed GF/F filters; blank values were subtracted from samples.

SXRF SAMPLE ANALYSIS

Samples for single-trichome SXRF analysis were prepared either with or without an oxalate-EDTA treatment to remove adsorbed Fe (Tovar-Sanchez et al., 2003). For the non-oxalate-treated samples, glutaraldehyde-fixed *Trichodesmium* colonies or single trichomes were removed from the centrifuge tube and pipetted in 10-μL drops onto LUX film-coated Cu TEM grids (Ted Pella, Redding, CA). In order to avoid the formation of salt crystals, seawater was delicately wicked from the grids using the corner of a Kimwipe. A 10-μL droplet of Milli-Q was then pipetted onto the grid and immediately removed from the grid using a Kimwipe.

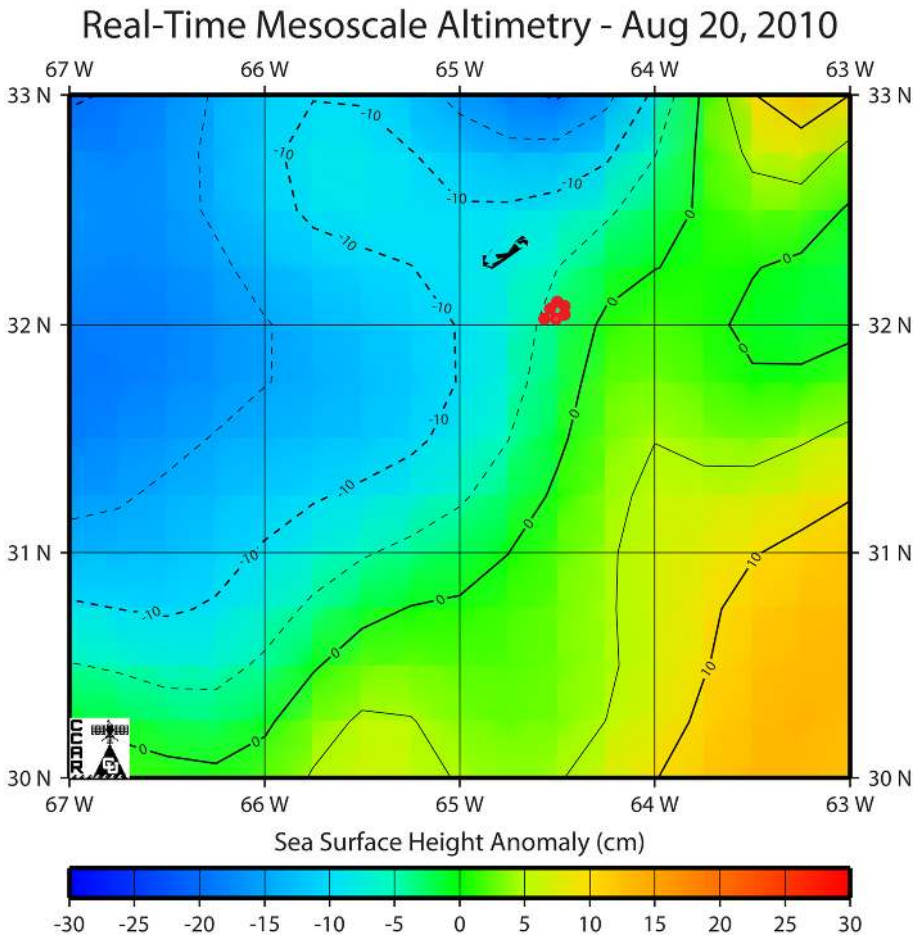

FIGURE 1 | Location of sampling stations in the Sargasso Sea overlaid on a map of sea surface height anomaly as determined by remote sensing from Jason, TOPEX/Poseidon, Geosat Follow-On, ERS-2 and Envisat satellites (Colorado Center for Astrodynamics Research, University of Colorado at Boulder; Leben et al., 2002). Bermuda can be seen to the northwest of the study region.

Table 1 | Summary of locations, sampling times, ambient temperature and salinity, and analyses performed.

Station	Latitude	Longitude	Local date	Local time	Temperature	Salinity	ICP-MS/CHN	SXRF (GSECARS)	SXRF (2ID-E)
1	32° 10′N	64° 30′W	8/19/10	14:30	n.d.	n.d.	4	n.d.	n.d.
2	31° 58′N	64° 17′W	8/19/10	23:00	28.9	36.7	3	n.d.	n.d.
3	31° 66′N	64° 17′W	8/20/10	8:00	28.5	36.7	4	9	n.d.
4	31° 66′N	64° 17′W	8/20/10	19:30	28.7	36.7	4	2	n.d.
5	31°70′N	64° 16′W	8/21/10	15:00	28.7	36.7	4	11	n.d.
7	31° 67′N	64° 17′W	8/22/10	12:00	28.8	36.7	n.d.	7	14

The number of replicate samples analyzed is listed for each technique. For inductively coupled plasma mass spectrometry (ICP-MS) and CHN analysis the number of replicate bulk colony assemblages analyzed is shown. For synchrotron x-ray fluorescence (SXRF) the number of trichome sections analyzed is shown. GSECARS and 2ID-E indicate the beamlines used to conduct SXRF analyses at the Advanced Photon Source.

The samples were then allowed to air dry in a laminar flow hood. For the oxalate-treated samples, a second batch of glutaraldehyde-fixed colonies were filtered onto 25-mm diameter 1-μm pore polycarbonate filter membranes under low vacuum pressure (< 50 mm Hg) and soaked for 15 min in trace-metal clean oxalate-EDTA reagent (Tovar-Sanchez et al., 2003). Soaked cells were subsequently rinsed three times with 0.8 mol L^{-1} ammonium formate solution isotonic to seawater. *Trichodesmium* colonies were then resuspended in fresh ammonium formate solution and individual colonies or trichomes were pipetted onto LUXfilm grids and allowed to air dry. Dried grids were stored in the dark until SXRF analysis.

Element concentrations and distributions within sections of trichomes were analyzed at the Advanced Photon Source (Argonne National Laboratory, Argonne, Il, USA) using hard x-ray microprobe beamlimes 2ID-E and GSECARS 13ID-C. The 2ID-E beamline allows for high-resolution imaging (ca. 0.4 μm FWHM) via a 10 keV x-ray beam focused with a Fresnel zone plate with a 320 micron diameter and 100 nm outermost zonewidth (X-radia, Inc, Plesanton, CA). The 13ID-C beamline uses Kirkpatrick-Baez mirrors to focus a larger beam (ca. 2 μm FWHM) useful for efficient scanning of larger areas. The lower resolution at GSECARS 13ID-C enables scanning of larger sections of trichomes at the expense of higher spatial resolution. Samples were analyzed at both beamlines inside a He-filled sample chamber to reduce background Ar fluorescence and maximize efficiency of detection of x-ray fluorescence originating from low-Z elements. At GSECARS samples were analyzed using a monochromatic 7.3 keV x-ray beam in order to improve sensitivity for elements of lower energy such as P and S.

Element quantification of spatial regions of interest (ROI; e.g., trichome section, background) within each trichome section was performed as described by Twining et al. (2011). Briefly, spectra of pixels belong to each ROI were averaged and fit using the software package MAPS (Vogt, 2003). A multi-element exponentially modified Gaussian peak model was used to convert peak areas to areal element concentrations using NBS-certified thin-film standards (SRM 1832 and SRM 1833). The conversion factor for the elements P and S which are not present in either SRM was obtained interpolating the conversion factor of other elements as a function of their theoretical fluorescence yield (Núñez-Milland et al., 2010). The areal element concentration of each trichome ROI was calculated after subtraction of a background ROI recorded in close proximity to the trichome ROI.

STATISTICAL TREATMENT

Phosphorous-normalized element stoichiometries for samples taken at different time points and measured using ICP-MS were compared using a non-parametric Kruskal–Wallis test (JMP 9, SAS Institute, Cary, NC, USA). As a subsample of SXRF samples was treated with an oxalate solution, a two-way ANOVA was used to test the significance of sampling time and oxalate treatment effects. As the oxalate and non-oxalate samples showed no significant difference ($p > 0.05$) for metal and S quotas, these data were subsequently grouped together, and temporal variability of S-normalized metal stoichiometries was tested using a non-parametric Kruskal–Wallis test.

RESULTS

ELEMENTAL CONTENT OF *TRICHODESMIUM* COLONIES

The bulk elemental content of *Trichodesmium* colonies was assessed by analyses of picked colonies (**Table 2**). The measurement of C and N on concurrent samples for each station allowed normalizing ICP-MS element signatures to these additional biomass proxies. Mean (± SD) C:N (6.03 ± 1.05 mol mol^{-1}) was slightly below the canonical Redfield ratio (6.7 mol mol^{-1}). However mean N:P ranged from 93 to 148 mol mol^{-1} at each station, and mean C:P was four- to seven-fold above the Redfield ratio of 106 mol mol^{-1} (**Table 2**), suggesting that cells were severely P-limited under the oligotrophic late-summer conditions present in the surface waters of the Sargasso Sea. Vanadium was the most abundant metal in the colonies (66–100 μmol mol^{-1} C), followed by Fe (21–40 μmol mol^{-1} C), Zn (6–29 μmol mol^{-1} C), Ni and Mo (9–17 μmol mol^{-1} C), and Mn and Cu (4–9 μmol mol^{-1} C; **Table 2**). Cadmium was approximately two orders of magnitude less abundant in *Trichodesmium* (0.01–0.12 μmol mol^{-1} C).

P- AND S-NORMALIZED METAL STOICHIOMETRIES

While C provides the most direct proxy for cell biomass, C was not measured on the exact same samples as trace metals due to the different analytical techniques required. Phosphorus, however, was measured on the same sample digests as the metals, so P-normalized metal stoichiometries are used to more precisely normalize metal contents to variations in colony biomass between the picked samples. Mean P content per colony

Table 2 | Mean element quotas measured by CHN and ICP-MS for *Trichodesmium* colonies collected from the Sargasso Sea.

Station	C	N	P	V	Mn	Fe	Ni	Cu	Zn	Mo	Cd	C:N	C:P	V:C	Mn:C	Fe:C	Ni:C	Cu:C	Zn:C	Mo:C	Cd:C
Blank	**12.9**	**3.85**	**n.d.**	**0.03**	**0.02**	**0.38**	**0.01**	**n.d.**	**n.d.**	**n.d.**	**n.d.**										
	6.58	*1.72*	*n.d.*	*0.01*	*0.01*	*0.15*	*0.01*														
1	**582**	**99.4**	**0.98**	**58.1**	**5.09**	**17.3**	**6.34**	**3.9**	**6.31**	**8.39**	**58.1**	**5.9**	**596**	**100**	**8.7**	**30**	**11**	**6.7**	**11**	**14**	**0.10**
	129	*24.6*	*0.28*	*n.d.*	*1.25*	*3.99*	*1.65*	*0.93*	*5.1*	*5.39*	*15.8*	*0.2*	*216*	*22*	*2.9*	*9.5*	*3.7*	*2.2*	*9.1*	*9.8*	*0.035*
2	**545**	**92.3**	**0.76**	**36.1**	**3.86**	**11.7**	**4.74**	**2.76**	**3.02**	**9.22**	**39.7**	**5.9**	**716**	**66**	**7.1**	**21**	**8.7**	**5.1**	**5.5**	**17**	**0.07**
	45.3	*6.75*	*0.32*	*17.6*	*1.59*	*2.61*	*1.84*	*1.61*	*0.94*	*4.87*	*37*	*0.2*	*282*	*33*	*3.0*	*5.1*	*3.4*	*3.0*	*1.8*	*9.0*	*0.068*
3	**633**	**97**	**1.34**	**57.4**	**5.83**	**22.2**	**9.58**	**3.56**	**13.31**	**6.43**	**72.9**	**6.8**	**474**	**91**	**9.2**	**35**	**15**	**5.6**	**21**	**10**	**0.12**
	194	*35.1*	*0.25*	*29*	*0.77*	*8.51*	*3.1*	*0.72*	*8.55*	*2.32*	*34.2*	*2.1*	*170*	*54*	*3.1*	*17*	*6.7*	*2.1*	*15*	*4.8*	*0.065*
4	**518**	**86.9**	**0.74**	**45.2**	**3.91**	**11.4**	**5.57**	**2.19**	**9.8**	**5.2**	**27.7**	**5.9**	**702**	**87**	**7.5**	**22**	**11**	**4.2**	**19**	**10**	**0.05**
	97.7	*12.6*	*0.12*	*7.7*	*0.52*	*2.86*	*1.11*	*0.28*	*8.2*	*1.05*	*9.39*	*0.3*	*173*	*22*	*1.7*	*6.9*	*3.0*	*1.0*	*16*	*2.8*	*0.021*
5	**379**	**67.9**	**0.74**	**32.9**	**3.43**	**15**	**5.94**	**2.3**	**11.08**	**6.08**	**31.8**	**5.6**	**514**	**87**	**9.1**	**40**	**16**	**6.1**	**29**	**16**	**0.08**
	47.5	*5.9*	*0.16*	*5.3*	*0.55*	*12.7*	*1.08*	*0.59*	*12.19*	*1.53*	*14*	*0.9*	*127*	*18*	*1.8*	*33.7*	*3.5*	*1.7*	*32*	*4.5*	*0.038*

*C, N, and P are in units of nmol·colony^{-1}; Fe, Zn, Mn, Cu, Ni, Mo, and V are in units of pmol·colony^{-1}, and Cd data are in units of fmol·colony^{-1}. C:N and C:P data are in units of mol mol^{-1}; Fe:C, Zn:C, Mn:C, Cu:C, Ni:C, Mo:C, Cd:C, and V:C in μmol mol^{-1}. Blanks were calculated by dividing the mean elemental content of blank digestion vials by the typical number of colonies per sample vial (n = 20). SD for C-normalized ratios were calculated by propagation of error. The number of replicate samples analyzed for each element is shown in **Table 1**. Mean, bold; SD, italics; n.d., below detection limit.*

varied 1.8-fold between stations (**Table 2**), but the P-normalized metal stoichiometries measured by ICP-MS follow the trends observed in the C-normalized stoichiometries (V:P > Fe:P > Zn:P ≈ Ni:P ≈ Mo:P > Mn:P ≫ Cd:P; **Table 3**).

Stoichiometries of several metals (Fe, Mn, V) were measured with both ICP-MS and SXRF in *Trichodesmium* collected from the same station, enabling direct comparisons between the techniques (**Figure 2**). Fe:P stoichiometries were generally comparable (10–25 mmol mol^{-1}), while Mn:P showed a systematic offset, with approximately threefold higher Mn:P measured in picked colonies with ICP-MS (4.4–5.3 mmol mol^{-1}) than measured in sections of trichomes with SXRF (1.1–1.7 mmol mol^{-1}). V:P stoichiometries were fairly constant in communities of picked *Trichodesmium* (41–63 mmol mol^{-1}) but were highly variable in subsections of the trichomes analyzed with SXRF, ranging more than 500-fold in trichomes collected from the same station. This complicates comparison between techniques. However, SXRF V:P stoichiometries were consistently higher than ICP-MS V:P stoichiometries at one station, consistently lower at another station, and spanned the ICP-MS stoichiometries at a third station, indicating that there was not a systematic offset in results between the techniques and that SXRF stoichiometries are a strong function of which trichome section is analyzed.

Sections of two *Trichodesmium* colonies were further analyzed at two different beamlines to examine variability on different spatial scales. The compatibility of the data from the two beamlines was assessed by comparing areal concentrations measured on the same trichome section. The overlapping regions of analysis are indicated for trichomes C and D in **Figures 3** and **4**, respectively. The areal concentrations for V, Mn, and Fe measured at GSECARS were consistently two- to five-fold below those measured in overlapping trichome sections at 2ID-E (**Figure 5**; **Table 4**). However

Table 3 | P-normalized mean metal stoichiometries of *Trichodesmium* measured by ICP-MS or SXRF.

Station	Technique	Time	V:P	Mn:P	Fe:P	Ni:P	Zn:P	Mo:P	Cd:P
1	ICP-MS	14:30	**50.4**	**5.4**	**20.0**	**6.5**	**8.0**	**8.7**	**64.9**
			1.4	*11.7*	*0.6*	*8.6*	*4.5*	*30.9*	
2	ICP-MS	23:00	**47.0**	**5.1**	**16.9**	**6.5**	**4.4**	**11.9**	**47.9**
			7.6	*0.6*	*5.9*	*1.5*	*1.2*	*3.1*	*37.0*
3	ICP-MS	8:00	**41.5**	**4.4**	**16.3**	**7.6**	**9.6**	**5.1**	**52.6**
			15.9	*0.5*	*4.3*	*5.3*	*0.2*	*2.5*	*17.2*
3	SXRF	8:00	**96**	**1**	**13**				
			30	*0.2*	*3.7*				
4	ICP-MS	19:30	**63.1**	**5.3**	**15.6**	**7.7**	**13.7**	**7.0**	**37.6**
			17.5	*0.7*	*4.4*	*1.9*	*12.7*	*0.7*	*12.6*
4	SXRF	19:30	**2.8**	**1.3**	**28.6**				
			3.9	0.5	25.9				
5	ICP-MS	15:00	**45.3**	**4.7**	**19.0**	**8.1**	**13.5**	**8.6**	**41.5**
			18.7	*0.3*	*12.2*	*1.1*	*12.5*	*2.8*	*10.6*
5	SXRF	15:00	**108**	**1**	**24**				
			235	*1*	*22*				
7	SXRF	12:00	**70**	**3**	**63**		**68**		
			43	*2*	*32*		*54*		

Cd:P stoichiometry is presented as umol mol^{-1} and Mo:P, V:P, Mn:P, Fe:P, Ni:P, and Zn:P data are presented as mmol mol^{-1}. Mean, bold; SD, italics. Only data for non-oxalate-washed trichomes or colonies are included.

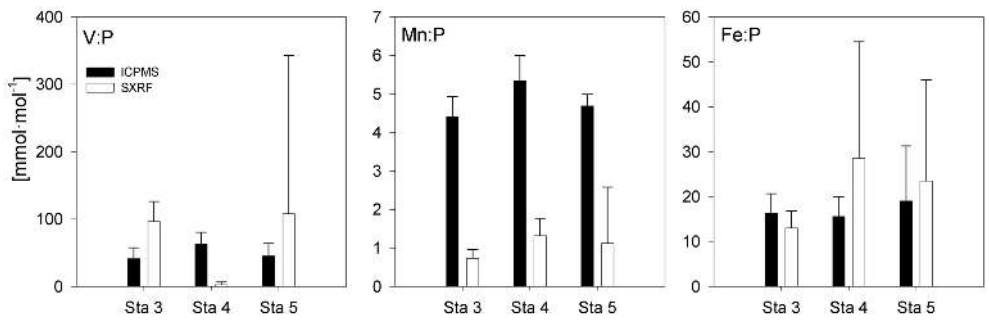

FIGURE 2 | P-normalized metal quotas of *Trichodesmium* as determined by ICP-MS and SXRF on samples collected at the same station. The bars are means ± SD for replicate filters (ICP-MS) or for different trichome sections in colonies collected from the same station (SXRF). Only data for non-oxalate-washed trichomes and colonies are included.

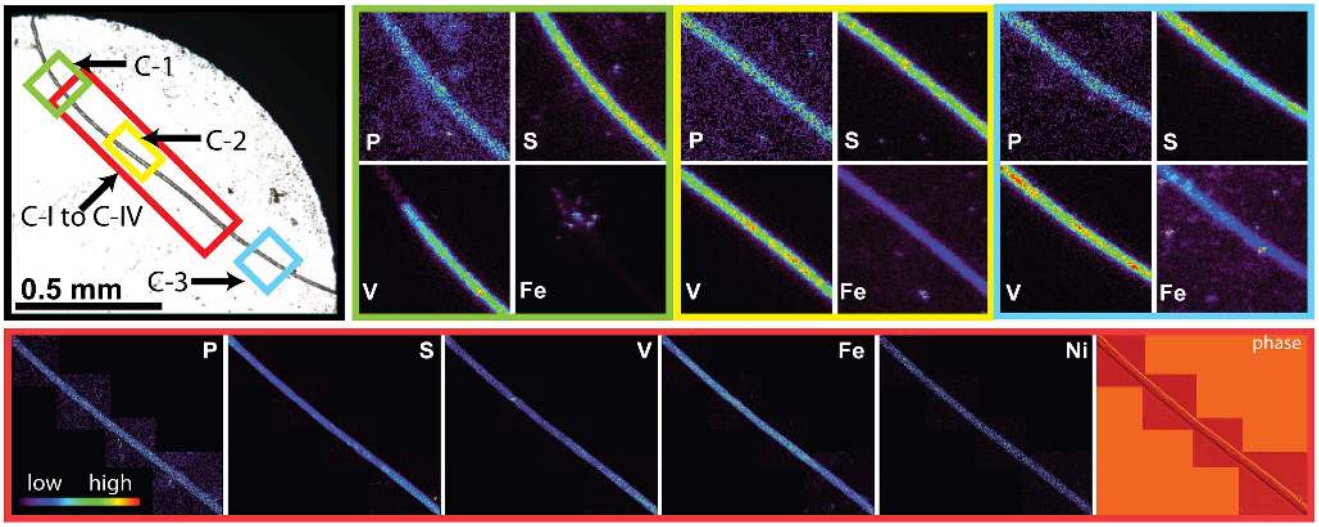

FIGURE 3 | Light micrographs, false-color element (P, S, V, Fe and Ni) maps, and differential phase contrast images (phase) (Hornberger et al., 2008) of *Trichodesmium* trichome C. The color scale for element maps is shown, with warmer colors indicating higher element concentrations. The color scheme of the differential phase contrast image does not follow the color scale for the element maps. The location of each trichome section is indicated on the light micrograph with a unique outline color. Maps C-1 (green), C-2 (yellow), and C-3 (blue) were recorded at the GSECARS beamline, while maps C-I to C-IV (red) were recorded at 2ID-E.

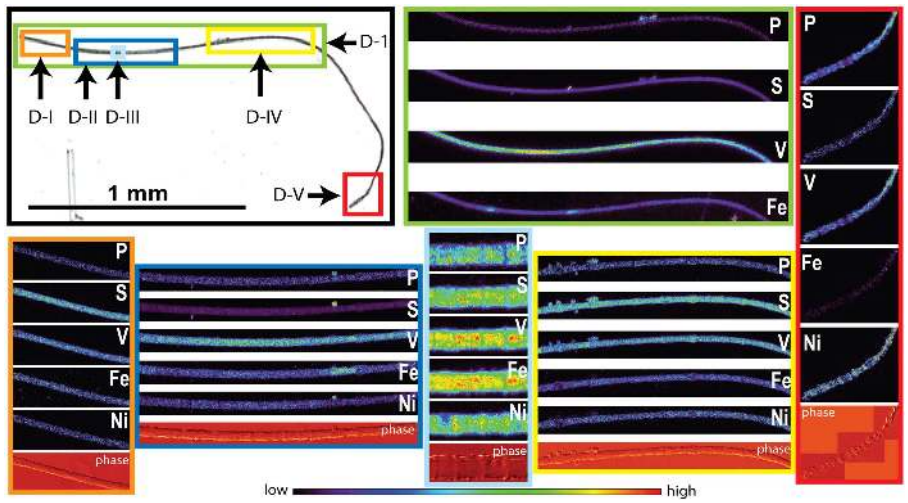

FIGURE 4 | Light micrographs, false-color element (P, S, V, Fe and Ni) maps, and differential phase contrast images (phase) (Hornberger et al., 2008) of *Trichodesmium* trichome D. The color scale for element maps is shown, with warmer colors indicating higher element concentrations. The color scheme of the differential phase contrast image does not follow the color scale for the element maps. The location of each trichome section is indicated on the light micrograph with a unique outline color. MAP D-1 (green) was recorded at the GSECARS beamline, while maps D-I (orange), D-II (dark blue), D-III (light blue), D-IV (yellow), and D-V (red) were recorded at 2ID-E.

metal concentrations normalized to biomass proxies P or S were generally comparable between beamlines (**Figure 5**).

A subset of the *Trichodesmium* colonies analyzed with SXRF was treated with an oxalate-EDTA solution to remove externally bound Fe, enabling comparisons between treated and untreated trichomes. Areal concentrations (nmol cm^{-2}) of S, Fe, Mn, and V were not significantly different in oxalate-treated trichome sections compared to non-oxalate-treated trichome sections (two-way ANOVA, $p > 0.267$), however least-square mean P concentrations were 47% lower in treated trichomes ($p = 0.012$; **Figure 6**). Due to the sparse *Trichodesmium* population encountered during the sampling campaign, the effect of an oxalate-EDTA treatment was only assessed for SXRF samples and not for ICP-MS and CHN samples.

Trichodesmium samples were collected at different times of day over the course of the cruise, and temporal differences were examined separately in the ICP-MS and SXRF datasets. Bulk ICP-MS P-normalized stoichiometries for non-oxalate-rinsed colonies

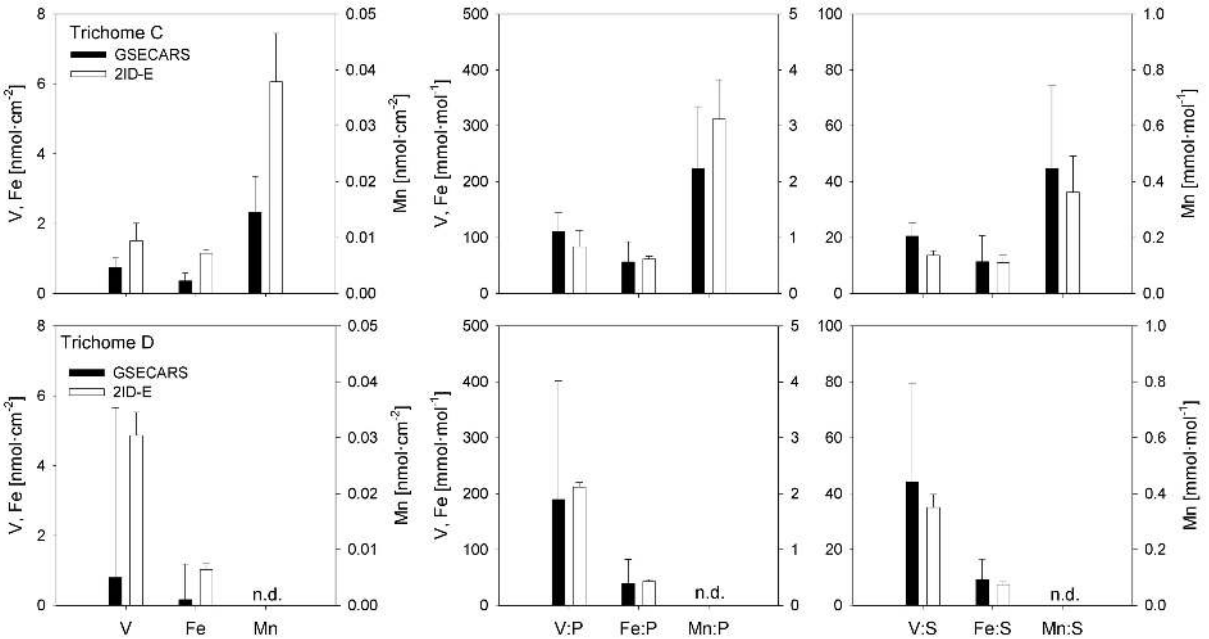

FIGURE 5 | Comparison of element concentrations in overlapping trichome sections analyzed with GSECARS and 2ID-E beamlines. The panels on the left present V, Fe, and Mn concentrations as nmol cm^{-2}. The four panels on the right present V, Fe, and Mn concentrations normalized to P (mmol mol^{-1}). The bars are means ± SD. n.d., concentrations below detection level.

Table 4 | Comparison of areal element concentrations and P- and S-normalized stoichiometries for V, Mn, and Fe measured at GSECARS and at 2ID-E.

	GSECARS										2ID-E								
Trichome	**V**	**Mn**	**Fe**	**V:P**	**Mn:P**	**Fe:P**	**V:S**	**Mn:S**	**Fe:S**	**Trichome**	**V**	**Mn**	**Fe**	**V:P**	**Mn:P**	**Fe:P**	**V:S**	**Mn:S**	**Fe:S**
C-1	1.02	0.01	0.24	143	1.62	33.3	25.7	0.29	5.97	C-I	2.08	0.03	1.06	116	2.85	56.3	15.5	0.23	7.86
C-2	0.47	0.02	0.61	75.5	3.51	98.4	17.0	0.79	22.12	C-II	1.27	0.05	1.17	74.4	3.92	67.0	13.1	0.49	12.1
C-3	0.72	0.01	0.23	112	1.56	36.5	18.8	0.26	6.10	C-III	1.16	0.03	1.22	59.8	2.59	60.8	12.1	0.36	12.8
D-1	0.80	n.d.	0.16	190	n.d.	39.3	44.2	n.d.	9.15	D-I	4.10	n.d.	0.88	209	n.d.	43.2	29.9	n.d.	6.41
										D-II	5.20	n.d.	1.21	205	n.d.	45.8	36.5	n.d.	8.45
										D-III	5.29	n.d.	0.97	221	n.d.	39.1	38.8	n.d.	7.14
										D-IV	3.49	n.d.	0.90	171	n.d.	42.4	26.3	n.d.	6.77

Areal concentrations are presented in nmol cm^{-2}, while P- and S-normalized data are presented in mmol mol^{-1}.

varied significantly with time only for Cu:P (Kruskal–Wallis test, $p = 0.042$), as variations in bulk V:P, Fe:P, Mn:P, Ni:P, Mo:P, Al:P, and Zn:P were not significant (**Figure 7**). Temporal variations in SXRF-analyzed trichomes were assessed with S-normalized stoichiometries due to the lack of an effect of oxalate on S; this allowed us to use all SXRF data in the comparison, increasing statistical power. Only Fe:S varied significantly with time (Kruskal–Wallis test, $p = 0.010$), with the highest Fe concentrations measured at noon (**Figure 8**). Bulk ICP-MS analyses could not be performed for the noon sampling station due to a lack of sufficient *Trichodesmium* biomass (**Table 1**), and this difference in the composition of the datasets likely explains the contrasting statistical results for the ICP-MS and SXRF data (as the highest Fe:P was observed at noon).

SPATIAL ELEMENT DISTRIBUTION WITHIN *TRICHODESMIUM* TRICHOMES

The spatial distribution of elements within *Trichodesmium* was studied using SXRF mapping at two different beamlines with different spatial resolution. The step size was 1.5 and 0.4 μm for GSECARS and 2ID-E, respectively. Element maps for P, S, V, Fe, and Ni were compared to each other and to light micrographs of the same trichome (**Figures 3–4**, **9–11**). The outline of the *Trichodesmium* trichomes is evident in both the light micrographs and the element maps. Phosphorus and S were generally more evenly distributed along trichomes than V and Fe (e.g., **Figures 3–4**, **9–11**). Where regions of Fe and V enrichment were observed, they typically did not overlap with each other. For example, in trichome section D-1 two zones of Fe enrichment are separated by a region of

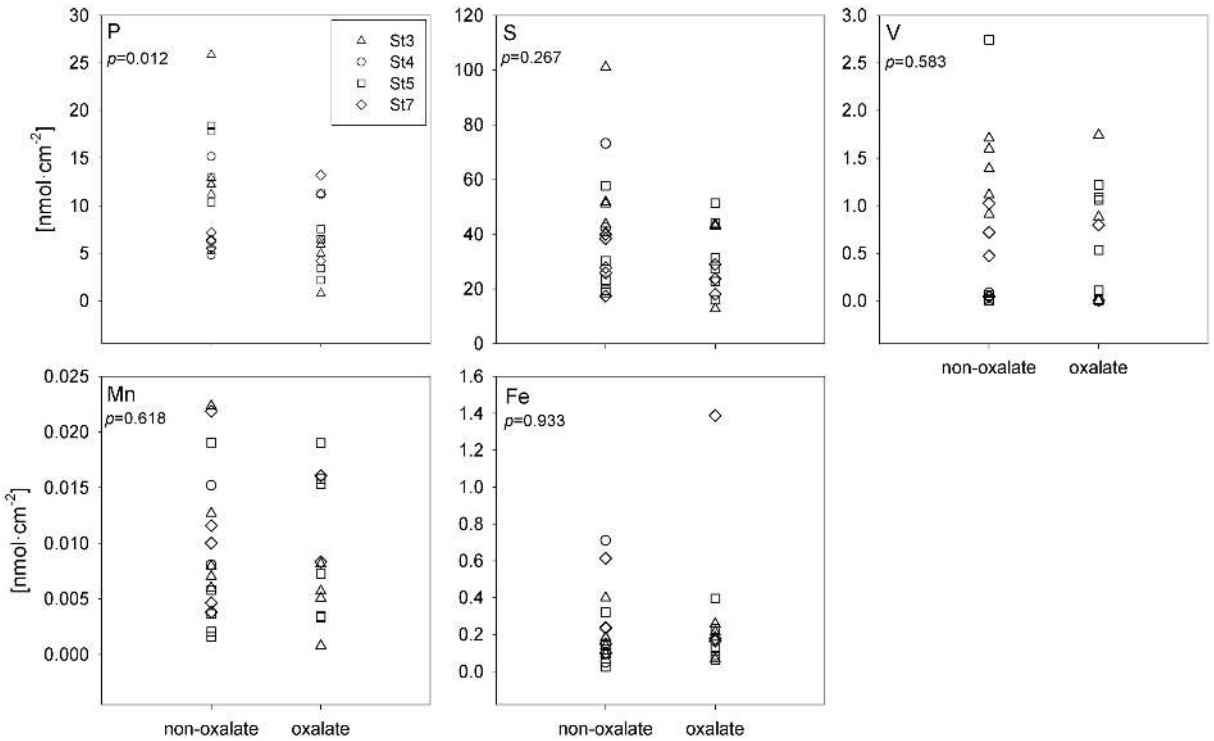

FIGURE 6 | Comparison of SXRF-analyzed trichome sections with or without oxalate treatment to remove externally bound elements. Areal concentrations are presented in nmol cm^{-2}. Each station has its unique symbol: St 3 – triangle, St 4 – circle, St 5 – square, and St 7 – diamond. The statistical significance of the effect of oxalate rinsing on the metal quotas (as determined with a two-way ANOVA; see text), is shown in each panel.

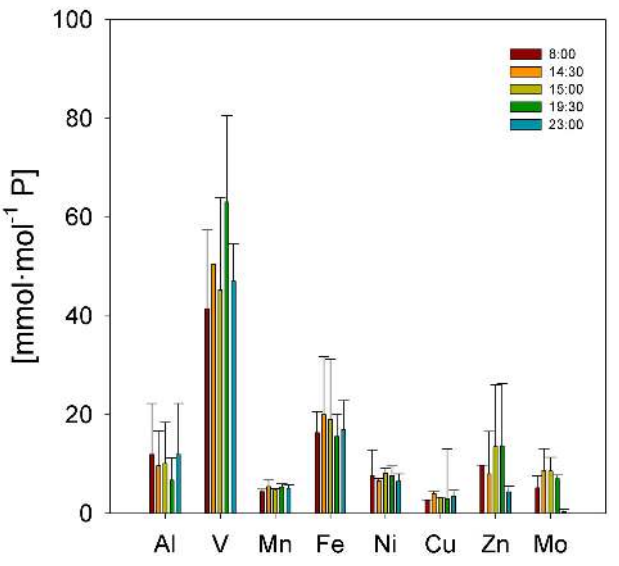

FIGURE 7 | Temporal comparison of P-normalized element quotas determined by ICP-MS for natural *Trichodesmium* populations. Bars are means ± SD.

elevated V in contiguous cells; this was confirmed at two separate beamlines (**Figure 4**). Other sections of the same trichome have very homogenous elemental distributions. While Fe enrichments zones were found in approximately 10% of trichomes, V was less uniformly distributed and zones of enrichment were observed in ca. 50% of trichomes (e.g., **Figure 3**, Map C-1, C-2). The high spatial variability of V and Fe seen in trichome D is shown quantitatively in a 1-D line plot presenting per-pixel concentrations along the main axis of trichome section D-1 (**Figure 12**). The high variability within a trichome is further illustrated by a comparison of the areal concentrations of P- and S-normalized metal stoichiometries calculated for different regions of interest within trichomes C and D using data from either GSECARS or 2ID-E (**Table 4**). Both V and Fe varied two- to three-fold between sections of the same trichome.

The higher incident x-ray energy used at 2ID-E also allowed us to map the Ni distribution within trichome sections. In contrast to V or Fe, Ni did not show notable enrichment in contiguous cells of a trichome. However the sub-cellular Ni distribution within a trichome differed from the distribution of other elements such as P, S, V, Mn, and Fe. While the concentrations of the latter elements were highest within each cell, Ni was most abundant in the membranes connecting the cells (**Figure 4**, Maps D-III and D-V). Such Ni distribution was not observed in trichome C (**Figure 3**).

DISCUSSION

It is widely acknowledged that diazotrophs such as *Trichodesmium* have high Fe quotas as a result of the biochemical demands of the nitrogenase enzyme (Raven, 1988; Berman-Frank et al., 2001; Kustka et al., 2003a), however elevated quotas of other metals in *Trichodesmium* that may result from their unique physiology have received less attention. This study documents elevated V,

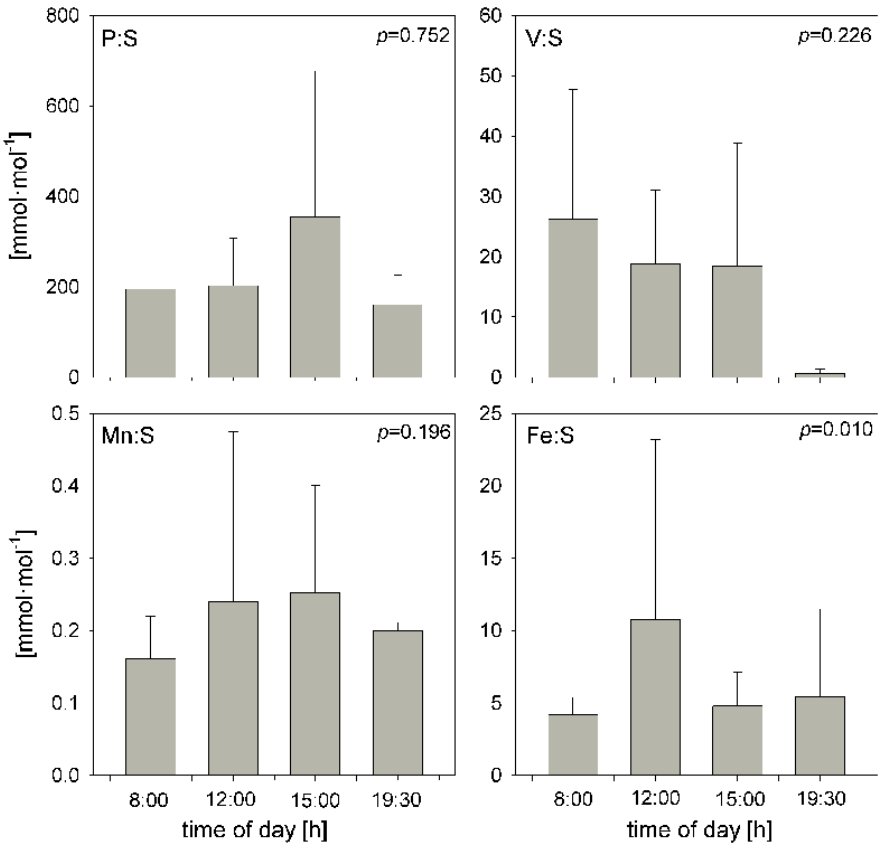

FIGURE 8 | Temporal comparison of S-normalized element stoichiometries determined with SXRF (combined oxalate and non-oxalate data from both beamlines) on individual trichome sections. Bars are means ± SD. The statistical significance of the effect of sampling time on the element stoichiometries (as determined with a non-parametric Kruskal–Wallis test; see text), is shown in each panel.

Ni, and Mo in *Trichodesmium* collected from the Sargasso Sea, utilizing both bulk and single-cell elemental analyses, and attempts to understand the causes of this unique elemental signature.

Studies of metal quotas in plankton typically present metal contents normalized to cell biomass. The major elemental constituents C and P are often used as somewhat interchangeable proxies of biomass (e.g., Bruland et al., 1991), however the *Trichodesmium* samples analyzed in this study were significantly depleted in P relative to C and N, and thus comparisons between these results and other studies will depend on the choice of biomass proxy. Previous studies have documented similar enrichments in cellular C and N, relative to P, in *Trichodesmium* from the Sargasso Sea and grown in culture under P-limited conditions (White et al., 2006; Orchard et al., 2010b), and Sañudo-Wilhelmy et al. (2001) argue that *Trichodesmium* in the North Atlantic can be limited by P availability. Phosphorus limitation of *Trichodesmium* is further indicated by the *Trichodesmium* N:P ratios, which were elevated above 50; this has been suggested as an indicator of P limitation (Geider and La Roche, 2002). In contrast, *Trichodesmium* collected from more P-replete waters near Western Australia presented a mean C:N:P ratio of 154:25:1 (Berman-Frank et al., 2001).

Comparisons to cellular S measured with SXRF also indicate that the *Trichodesmium* were depleted in P. Sulfur is incorporated into cells primarily via cysteine and methionine and has been used as an additional biomass proxy in previous SXRF studies (Twining et al., 2004, 2011; King et al., 2011). Phosphorus:sulfur ratios in P-replete cells experiencing elementally balanced growth are typically close to 1 (Payne and Price, 1999; Ho et al., 2003; Twining et al., 2011), but P:S reported here for *Trichodesmium* are approximately three- to six-fold below this (**Table 5**). *Trichodesmium* is able to substitute non-P sulfolipids for phospholipids under P limitation (Van Mooy et al., 2009), and this may also contribute to the reduced P:S stoichiometries.

Irregardless of the choice of biomass proxy, comparisons to published data clearly indicate that the *Trichodesmium* in this study have elevated V, Mo, and Ni contents. In most non-diazotrophic taxa Fe is generally the most abundant metal, followed by Zn, Mn, Ni, Cd, and Mo (Bruland et al., 1991; Sunda and Huntsman, 1995, 2000; Ho et al., 2003; Twining et al., 2011). In contrast, V was found to be the most abundant metal in *Trichodesmium*, with the mean V quota exceeding the mean Fe quota by threefold. While less abundant than Fe (and V), C-normalized Mo, and Ni quotas were approximately 50- and 3-fold higher in *Trichodesmium* than in previously studied non-diazotrophs (Ho et al., 2003; Twining et al., 2011). Indeed, Mo and Ni were present at levels similar to that of Zn, which is usually at least three times more abundant than these metals in phytoplankton (Bruland et al., 1991;

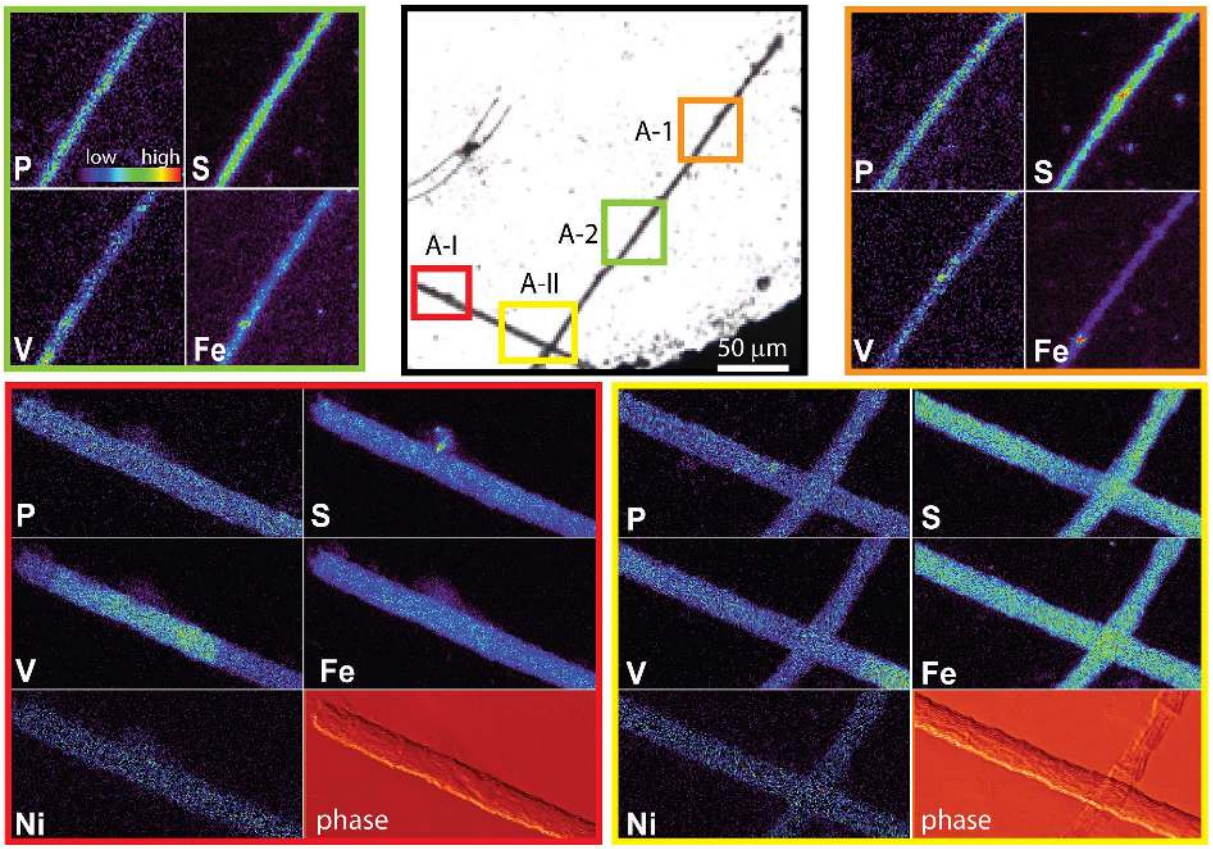

FIGURE 9 | Light micrographs, false-color element (P, S, V, Fe and Ni) maps, and differential phase contrast images (phase) (Hornberger et al., 2008) of a *Trichodesmium* trichome. The color scale for element maps is shown, with warmer colors indicating higher element concentrations. The color scheme of the differential phase contrast image does not follow the color scale for the element maps. The location of each analyzed trichome section is indicated on the light micrograph. MAP A-1 (orange) and map A-2 (green) were recorded at the GSECARS beamline, while maps A-I (red) and A-II (yellow) were recorded at 2ID-E.

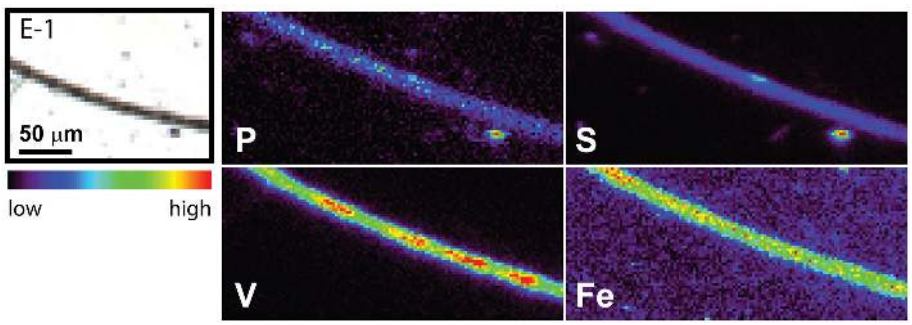

FIGURE 10 | Light micrographs and false-color element (P, S,V, and Fe) maps of a *Trichodesmium* trichome. The color scale for element maps is shown, with warmer colors indicating higher element concentrations. The trichome section E-1 shown in the light micrograph was analyzed at GSECARS.

Twining et al., 2011). Given the depressed P contents of the trichomes, P-normalized quotas of V, Fe, Zn, Mn, Ni, and Mo are also higher than has been observed in other groups of phytoplankton (Bruland et al., 1991; Ho et al., 2003; Twining et al., 2011). The present results are in agreement with previous studies on field populations of *Trichodesmium* collected from the western sub-tropical North Atlantic (Tovar-Sanchez et al., 2006; Tovar-Sanchez and Sañudo-Wilhelmy, 2011), which also showed high cellular V, Mo, and Ni quotas. However, V stoichoimetries reported here are at least 10-fold higher than measured in *Trichodesmium* from the other regions (Tovar-Sanchez et al., 2006; Tovar-Sanchez and Sañudo-Wilhelmy, 2011).

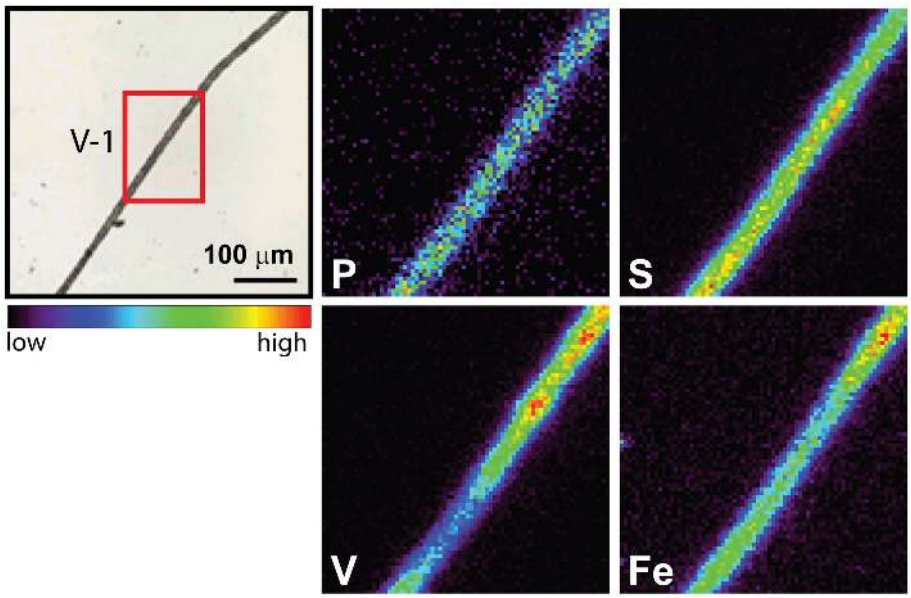

FIGURE 11 | Light micrographs and false-color element (P, S,V, and Fe) maps of a *Trichodesmium* trichome. The color scale for element maps is shown, with warmer colors indicating higher element concentrations. The location of the analyzed trichome section is indicated on the light micrograph in red (V-1). This map was recorded at GSECARS.

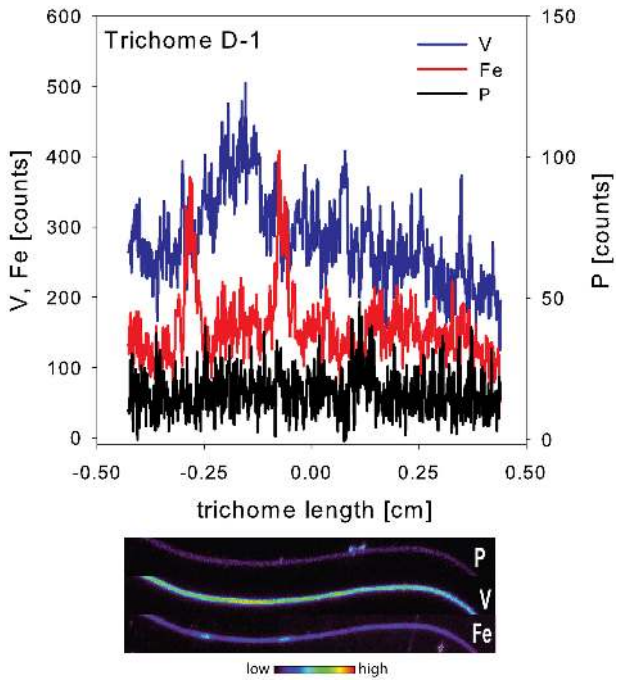

FIGURE 12 | One dimensional line plot along the main axis of trichome D-1. Data were extracted from the entire visible section of the trichome mapped here. Associated elemental maps of P, V, and Fe are given below.

Table 5 | Comparison of S-normalized stoichiometries for P, V, Mn, and Fe measured at GSECARS and at 2ID-E.

Time	P:S	V:S	Mn:S	Fe:S
8:00	**196**	**26.2**	**0.16**	**4.15**
	81.0	*21.5*	*0.06*	*1.22*
12:00	**203**	**18.8**	**0.24**	**11.0**
	108	*12.6*	*0.24*	*12.7*
15:00	**355**	**18.4**	**0.25**	**4.78**
	323	*20.5*	*0.15*	*2.36*
19:30	**160**	**0.57**	**0.20**	**5.43**
	65.9	*0.80*	*0.01*	*6.05*

Data are presented in mmol mol^{-1}. Mean, bold; SD: italics.

This unique elemental signature of *Trichodesmium* does not appear to result from external non-cellular material attached to the cells. As the Sargasso Sea receives atmospheric deposition of aerosols of anthropogenic origin due to fossil fuel combustion in North America, adsorbed dust particles are a possible cause of apparent increased quotas. Such combustion-derived aerosols are enriched in V and Ni in comparison to soil-derived dust particles (Sholkovitz et al., 2009). However only a few of the non-oxalate rinsed trichome sections analyzed by SXRF had localized V hotspots which do not correspond to the structure of contiguous cells within a trichome (**Figure 3** C-I to C-IV). Similar Fe hotspots were also detected in a few trichomes (**Figure 3** Map C-1 and C-3), but these hotspots do not drive the higher V and Fe quotas of the trichomes. Removing the pixels containing these potential external particles reduces the V and Fe quotas by less than 5%. Further, because V, Fe, and Ni do not co-localize in these hotspots, an anthropogenic origin for these particles is unlikely. Rather, it is likely that the particles are lithogenic. Recent work by Rubin et al. (2011) indicates that *Trichodesmium* may process

particulate Fe associated with colonies to obtain Fe. However, given that Fe:P ratios were comparable in analyzed colonies and individual trichomes, and that the Fe hotspots observed on the trichomes did not contribute significantly to their Fe content, it does not appear that external particles associated with colonies were a significant contributor to *Trichodesmium* elemental composition in this study. Although significant populations of metazoa, protozoa, algae, and bacteria may be associated with *Trichodesmium* colonies (Sheridan et al., 2002; Hewson et al., 2009), efforts were made to avoid these through manual isolation of individual colonies. The comparable Fe results for colonies and individual trichomes again suggest that such organisms, if present, also did not contribute significantly to the elemental content of the *Trichodesmium*.

Results from the oxalate rinse also indicate that the elevated metal quotas are not due to extracellular material. A comparison of the areal concentrations (nmol cm^{-2}) for oxalate and non-oxalate-treated cells from each station reveals that neither Fe and V, nor Mn and S, varied significantly between rinse treatments. To what extend this oxalate rinse can remove other elements such as V, Mn, or S has not been studied in detail. Although the oxalate treatment was developed to remove externally adsorbed Fe (Tovar-Sanchez et al., 2003), we observed P removal of up to 47% from oxalate-treated trichome sections; this matches previous reports of oxalate usage with *Trichodesmium* (Sañudo-Wilhelmy et al., 2004). The SXRF samples were fixed with glutaraldehyde prior to rinsing, and this could have impacted the lability of internal P as well (Tang and Morel, 2006), but other studies with unfixed *Trichodesmium* have reported even higher P removal with oxalate (Tovar-Sanchez and Sañudo-Wilhelmy, 2011). Overall the oxalate treatment did not affect the areal metal concentrations of *Trichodesmium* significantly, and we conclude that the influence of adsorbed lithogenic material on the quotas is insignificant.

While increased cell quotas do not necessarily indicate increased biological requirements, the elevated quotas of V, Fe, and Mo may result from *Trichodesmium*'s biochemical machinery, including metalloenzymes related to the demands of N fixation. Nitrogen fixation is enabled by the expression of the metalloenzyme nitrogenase. There are three known metallotypes of nitrogenase, containing either Mo and Fe (MoFe), V and Fe (FeV), or Fe only (FeFe; Bothe et al., 2010). Each type of nitrogenase requires a specific nitrogenase reductase (i.e., nifH, vnfH, and anfH, respectively) which is properly redox-tuned to the corresponding nitrogenase, as well as a suite of other proteins for proper enzyme assembly. While it is tempting to explain the V contents of *Trichodesmium* through expression of FeV nitrogenase, the *Trichodesmium erythraeum* genome lacks the δ subunit encoded by vnfG which is thought to be required for V-dependent N fixation (Eady, 2003; and references therein). Furthermore, in *Azotobacter vinelandii*, a model bacterium containing all three metallotypes of nitrogenase, nifDK (encoding for the MoFe protein) is universally expressed in the presence of MoFe whereas vnfDGK (encoding for FeV protein) is expressed only under low Mo conditions or under cooler temperatures. Neither condition applies to the Sargasso Sea, suggesting little if any selective pressure toward a V-dependent N fixation pathway in *Trichodesmium*. Given the high and nearly conservative concentrations of Mo in seawater (ca. 100 nM), the high intracellular Mo quotas measured here, and the lack of spatial or temporal correlations of V and Fe in cells, it appears that the nitrogenase enzyme is likely responsible for the elevated Fe and Mo contents – but not the elevated V contents – of *Trichodesmium*.

The high V content of *Trichodesmium* may instead result from the presence of other V-dependent metalloenzymes. Vanadium can also serve as a cofactor in haloperoxidases, and vanadium haloperoxidases (VHPO) have been structurally characterized for marine red (*Corallina officialis*) and brown (*Ascophyllum nodosum)* algae, as well as in the fungi *Curvularia inaequalis* (reviews in Crans et al., 2004; Winter and Moore, 2009). If expressed, such VHPOs may act as an antioxidant and help neutralize reactive oxygen species such as hydrogen peroxide (Drábková et al., 2006, 2007). Hydrogen peroxide is a by-product of photosynthesis (Bienert et al., 2006) and is especially damaging to the nitrogenase enzyme (Fay, 1992). An antioxidant role of VHPOs in *Trichodesmium* would be especially beneficial because *Trichodesmium* fixes N during daylight, and neutralizing reactive oxygen species by VHPOs might help facilitate simultaneously fixation of C and N. Johnson et al. (2011) recently described a 68 kDa VHPO encoded in the genome of the coastal cyanobacterium *Synechococcus* CC9311 and demonstrated the protein's capacity for bromoperoxidase activity. As homologs were only present in one other sequenced *Synechococcus* genome, they suggested this may be the result of a recent horizontal gene transfer event into *Synechococcus*. The *T. erythraeum* genome contains a putative acid phosphatase/vanadium-dependent haloperoxidase related protein (Accession number ABG53180). However the putative *Trichodesmium* protein, predicted to be 151 amino acids long (16.6 kDa), is much smaller than the well-characterized 609 amino acid (67.5 kDa) VHPO from *Curvularia inaequalis* (Accession CAA59686.1; Simons et al., 1995), and the *T. erythraeum* protein does not align with the region of the *C. inaequalis* protein that contains the amino acids required for activity (Hemrika et al., 1999). At this point, genomic evidence for either a V-dependent nitrogenase or a V-dependent HPO (with amino acids known to coordinate V in other VHPOs) is lacking. However, there are numerous metalloproteins in prokaryotes, including those that incorporate V, that have yet to be identified (Cvetkovic et al., 2010).

Vanadium could also be accumulated unintentionally by *Trichodesmium* via phosphate uptake mechansisms. If not complexed by siderophore-like compounds (Bellenger et al., 2007, 2011), V is expected to be present primarily as HVO_4^{2-} at pH 8 under oxic conditions (Crans et al., 2004). Vanadate and phosphate are similar in structure and electronic properties, but phosphate is more inert and not involved in redox transformations (Crans et al., 2004). Given that *Trichodesmium* populations are sometimes P-limited in the North Atlantic (Sañudo-Wilhelmy et al., 2001; Mills et al., 2004) it is intriguing to speculate that vanadate acquisition may occur under vanishingly low phosphate concentrations. Arsenate is taken up by phytoplankton via phosphate transporters (Oremland and Stolz, 2003), and As reduction (which follows uptake) is correlated with chlorophyll concentrations in the western North Atlantic (Cutter et al., 2001). While a P dependence of arsenate uptake has not been confirmed at the ultra-low phosphate concentrations characteristic of the Sargasso Sea (Foster et al., 2008), it is quite plausible that V may be taken up through this mechanism. It is interesting to note that the spatial distributions of V and P in the trichomes are not identical (**Figures 3–4**, **9–11**). The difference in cellular allocation may reflect redox reactions or other intracellular sequestration of V following uptake.

In order to allow for N fixation in the non-heterocystous cyanobacterium *Trichodesmium* spatial and temporal separation strategies are thought to separate the oxygen sensitive nitrogenase enzyme from the photosynthesis machinery (Berman-Frank, 2001; Berman-Frank et al., 2007; Finzi-Hart et al., 2009). Some trichomes collected at noon in this study showed the presence of contiguous cells enriched in Fe. In some samples these regions of elevated Fe were not evenly distributed over the whole trichome but were localized to zones separated by regions enriched in V (**Figures 4**, **11–12**). Such zones of Fe enrichment appear similar to the diazocytes identified in *Trichodesmium* (El-Shehawy, 2003; Sandh et al., 2011) and may represent zones of N fixation. In addition, such Fe enrichment zones in *Trichodesmium* were only observed for trichomes collected at noon. Interestingly, the mean Fe:P ratio for *Trichodesmium* samples collected at noon was significant higher than at any other sampling time. This is in agreement with the hypothesis that the onset of N fixation follows C fixation at midday (Finzi-Hart et al., 2009) and the highest expression of nifH (El-Shehawy, 2003).

The enrichment of Ni in *Trichodesmium* biomass likely also follows from biochemical usage. Nickel shows a distinctive spatial distribution with the highest concentration in the transverse wall membrane of *Trichodesmium* trichomes. Such distribution is in agreement with Ni containing membrane-bound enzymes such as urease (Collier et al., 1999), NiFe uptake hydrogenase (Tamagnini et al., 2002), and Ni-superoxide dismutase (Ni-SOD; Dupont et al., 2008b). SOD provides an important defense tool against the toxicity of superoxide by converting superoxide to molecular oxygen and hydrogen peroxide (McCord and Fridovich, 1969; Fridovich, 1989). Hydrogen peroxide is then further converted to water by peroxidases such as the previously described VHPOs (Crans et al., 2004). All aerobic organisms contain at least one isoform of SOD (containing either Fe, Mn, Cu/Zn, or Ni) with *Trichodesmium* containing the gene coding for Ni-SOD and Mn-SOD (Dupont et al., 2008a). Such mechanism is beneficial for *Trichodesmium* as the 4Fe-4S cluster in the nitrogenase complex is highly susceptible to the inactivation of superoxide. As H_2 is a side product of N fixation, all diazotrophic organisms contain NiFe hydrogenases (Tamagnini et al., 2002). In general these are divided into four groups, of which cyanobacteria have an uptake hydrogenase clustering together with cytoplasmic H_2 sensors and a bidirectional hydrogenase. While the bidirectional hydrogenase enzyme probably plays a role in fermentation or in electron transfer processes during photosynthesis, the uptake NiFe hydrogenase rapidly catalyzes H_2 produced during N fixation (Tamagnini et al., 2007). Only genes belonging to the uptake hydrogenase have been confirmed in *Trichodesmium* (Tamagnini et al., 2007). In addition to SOD and NiFe hydrogenases, the genome of *Trichodesmium* revealed the presence of a urease subunit alpha, subunit beta, and subunit gamma (Dupont et al., 2008a). *Trichodesmium* is able to grow on urea and as well on nitrate and ammonia (LaRoche and Breitbarth, 2005; Post et al., 2012), however urea is unlikely to be a significant source of N to *Trichodesmium* in the Sargasso Sea in the late summer (Orcutt et al., 2001). Thus it is unlikely that urease is driving the elevated Ni quotas of *Trichodesmium*. Rather, Ni is likely primarily incorporated into membrane enzymes such as Ni-SOD and NiFe hydrogenase.

Zinc contents of *Trichodesmium* may also be explained by usage in metalloenzymes. It has been suggested that cyanobacteria evolved under sulfidic conditions of low Zn availability that has resulted in lower Zn contents of modern cyanobacteria (Saito et al., 2003). In contrast, the elevated Zn quotas of *Trichodesmium* reported here may reflect the P-limiting condition of the Sargasso Sea and the subsequent expression of the Zn metalloenzyme alkaline phosphatase in *Trichodesmium*, as would be expected in cells growing on organic P substrates (Orchard et al., 2010a,b). Similarly, *Synechoccocus* in the Sargasso Sea increases its Zn quota substantially in anticyclonic eddies characterized by reduced phosphate delivery (Twining et al., 2010).

The Redfield ratio, and the proposed extension of this concept to include bioactive metals, is based on consistency of the *average* elemental composition of plankton. Indeed there is remarkable agreement in the bulk C:N:P ratios of plankton when data are aggregated (Geider and La Roche, 2002, and references therein), and compilations of selected bulk particulate metal studies have produced relative agreement (Bruland et al., 1991; Ho, 2006). However it has also been demonstrated that there is real and important spatial and taxonomic variability in the macronutrient and trace metal stoichiometries of plankton which underlie the average ratios (e.g., Geider and La Roche, 2002; Twining et al., 2004, 2011). Hence, a unified element stoichiometry should always be treated as a "statistical composition" (Redfield, 1958; Geider and La Roche, 2002). There is much to be learned about cell physiology, ecology and biogeochemistry from comparisons of plankton representing individual taxa and regions to the average elemental composition. The natural *Trichodesmium* populations described in this paper provide an example of how the physiology of an individual group, as well as the environmental conditions, can cause significant deviations from the averaged, idealized stoichiometric composition. The extent to which the unique elemental composition of *Trichodesmium* will impact nutrient and metal cycling in the surrounding waters will depend on the fate of the accumulated cell biomass. Future studies which combine elemental analyses of plankton with "-omics" approaches that constrain the genetic and biochemical composition of the same communities and populations will do much to advance our understanding of biogeochemistry in the ocean.

ACKNOWLEDGMENTS

We are grateful to the captain and crew of the R/V Atlantic Explorer and the staff of the Bermuda Atlantic Time-Series at Bermuda Institute of Ocean Sciences for enabling sample collection during cruise B-261. ICP-MS analyses were assisted by Mike Handley at the Orono campus of the University of Maine. CHN analyses were performed by Kathleen Thornton at the Darling Marine Center of the University of Maine. Conor Maginn and Sara Rauschenberg helped with SXRF analyses of *Trichodesmium* samples at the Advanced Photon Source. This work was supported by grants from the National Science Foundation to BST (OCE 0913080, OCE 0928289, and OCE 1061545). Use of the Advanced Photon Source, an Office of Science User Facility operated for the U.S. Department of Energy (DOE) Office of Science by Argonne National Laboratory, was supported by the U.S. DOE under Contract No. DE-AC02-06CH11357.

REFERENCES

Arrigo, K. R. (2005). Marine microorganisms and global nutrient cycles. *Nature* 437, 349–355.

Bellenger, J. P., Arnaud-Neu, F., Asfari, Z., Myneni, S. C. B., Stiefel, E. I., and Kraepiel, A. M. L. (2007). Complexation of oxoanions and cationic metals by the biscatecholate siderophore azotochelin. *J. Biol. Inorg. Chem.* 12, 367–376.

Bellenger, J. P., Wichard, T., Xu, Y., and Kraepiel, A. M. L. (2011). Essential metals for nitrogen fixation in a free-living N2-fixing bacterium: Chelation, homeostasis and high use efficiency. *Environ. Microbiol.* 13, 1395–1411.

Berman-Frank, I. (2001). Segregation of nitrogen fixation and oxygenic photosynthesis in the marine cyanobacterium Trichodesmium. *Science* 294, 1534–1537.

Berman-Frank, I., Cullen, J. T., Shaked, Y., Sherrell, R. M., and Falkowski, P. G. (2001). Iron availability, cellular iron quotas, and nitrogen fixation in Trichodesmium. *Limnol. Oceanogr.* 46, 1249–1260.

Berman-Frank, I., Quigg, A., Finkel, Z. V., Irwin, A. J., and Haramaty, L. (2007). Nitrogen-fixation strategies and Fe requirements in cyanobacteria. *Limnol. Oceanogr.* 52, 2260–2269.

Bienert, G. P., Schjoerring, J. K., and Jahn, T. P. (2006). Membrane transport of hydrogen peroxide. *Biochim. Biophys. Acta* 1758, 994–1003.

Bothe, H., Schmitz, O., Yates, M. G., and Newton, W. E. (2010). Nitrogen fixation and hydrogen metabolism in cyanobacteria. *Microbiol. Mol. Biol. Rev.* 74, 529–551.

Bruland, K. W., Donat, J. R., and Hutchins, D. A. (1991). Interactive influences of bioactive trace metals on biological production in oceanic waters. *Limnol. Oceanogr.* 36, 1555–1577.

Collier, J. L., Brahamsha, B., and Palenik, B. (1999). The marine cyanobacterium Synechococcus sp. WH7805 requires urease (urea amiohydrolase, EC 3.5.1.5) to utilize urea as a nitrogen source: molecular-genetic and biochemical analysis of the enzyme. *Microbiology* 145, 447–459.

Crans, D. C., Smee, J. J., Gaidamauskas, E., and Yang, L. (2004). The chemistry and biochemistry of vanadium and the biological activities exerted by vanadium compounds. *Chem. Rev.* 104, 849–902.

Cutter, G. A., Cutter, L. S., Featherstone, A. M., and Lohrenz, S. E. (2001). Antimony and arsenic biogeochemistry in the western Atlantic Ocean. *Deep Sea Res. Part II Top. Stud. Oceanogr.* 48, 2895–2915.

Cvetkovic, A., Menon, A. L., Thorgersen, M. P., Scott, J. W., Poole Ii, F. L., Jenney, F. E. Jr., Lancaster, W. A., Praissman, J. L., Shanmukh, S., Vaccaro, B. J., Trauger, S. A., Kalisiak, E., Apon, J. V., Siuzdak, G., Yannone, S. M., Tainer, J. A., and Adams, M. W. W. (2010). Microbial metalloproteomes are largely uncharacterized. *Nature* 466, 779–782.

Dominic, B., Zani, S., Chen, Y.-B., Mellon, M. T., and Zehr, J. P. (2000). Organization of the nif genes of the nonheterocystous cyanobacterium Trichodesmium Sp. IMS101. *J. Phycol.* 36, 693–701.

Drábková, M., Admiraal, W., and Maršálek, B. (2006). Combined exposure to hydrogen peroxide and light – selective effects on cyanobacteria, green algae, and diatoms. *Environ. Sci. Technol.* 41, 309–314.

Drábková, M., Matthijs, H., Admiraal, W., and Maršálek, B. (2007). Selective effects of H2O2 on cyanobacterial photosynthesis. *Photosynthetica* 45, 363–369.

Dupont, C. L., Barbeau, K., and Palenik, B. (2008a). Ni uptake and limitation in marine Synechococcus strains. *Appl. Environ. Microbiol.* 74, 23–31.

Dupont, C. L., Neupane, K., Shearer, J., and Palenik, B. (2008b). Diversity, function and evolution of genes coding for putative Ni-containing superoxide dismutases. *Environ. Microbiol.* 10, 1831–1843.

Eady, R. R. (2003). Current status of structure function relationships of vanadium nitrogenase. *Coord. Chem. Rev.* 237, 23–30.

El-Shehawy, R. (2003). Diurnal expression of hetR and diazocyte development in the filamentous nonheterocystous cyanobacterium Trichodesmium erythraeum. *Microbiology* 149, 1139–1146.

Fay, P. (1992). Oxygen relations of nitrogen fixation in cyanobacteria. *Microbiol. Rev.* 56, 340–373.

Finzi-Hart, J. A., Pett-Ridge, J., Weber, P. K., Popa, R., Fallon, S. J., Gunderson, T., Hutcheon, I. D., Nealson, K. H., and Capone, D. G. (2009). Fixation and fate of C and N in the cyanobacterium Trichodesmium using nanometer-scale secondary ion mass spectrometry. *Proc. Natl. Acad. Sci. U.S.A.* 106, 6345–6350.

Foster, S., Thomson, D., and Maher, W. (2008). Uptake and metabolism of arsenate by anexic cultures of the microalgae Dunaliella tertiolecta and Phaeodactylum tricornutum. *Mar. Chem.* 108, 172–183.

Fridovich, I. (1989). Superoxide dismutases. An adaptation to a paramagnetic gas. *J. Biol. Chem.* 264, 7761–7764.

Geider, R. J., and La Roche, J. (2002). Redfield revisited: Variability of C:N:P in marine microalgae and its biochemical basis. *Eur. J. Phycol.* 37, 1–17.

Haraguchi, H. (2004). Metallomics as integrated biometal science. *J. Anal. At. Spectrom.* 19, 5.

Hemrika, W., Renirie, R., Macedo-Ribeiro, S., Messerschmidt, A., and Wever, R. (1999). Heterologous expression of the vanadium-containing chloroperoxidase from Curvularia inaequalis in Saccharomyces cerevisiae and site-directed mutagenesis of the active site residues His496, Lys353, Arg360, and Arg490. *J. Biol. Chem.* 274, 23820–23827.

Hewson, I., Poretsky, R. S., Dyhrman, S. T., Zielinski, B., White, A. E., Tripp, H. J., Montoya, J. P., and Zehr, J. P. (2009). Microbial community gene expression within colonies of the diazotroph, Trichodesmium, from the Southwest Pacific Ocean. *ISME J.* 3, 1286–1300.

Ho, T. Y. (2006). "The trace metal composition of marine microalgae in cultures and natural assemblages," in *Algal Cultures, Analogues of blooms and Applications*, ed. D. V. Subba Rao. (Enfield, NH: Science Publishers).

Ho, T. Y., Quigg, A., Finkel, Z. V., Milligan, A. J., Wyman, K., Falkowski, P. G., and Morel, F. M. M. (2003). The elemental composition of some marine phytoplankton. *J. Phycol.* 39, 1145–1159.

Hornberger, B., De Jonge, M. D., Feser, M., Holl, P., Holzner, C., Jacobsen, C., Legnini, D., Paterson, D., Rehak, P., Struder, L., and Vogt, S. (2008). Differential phase contrast with a segmented detector in a scanning X-ray microprobe. *J. Synchrotron Radiat.* 15, 355–362.

Ji, Y., and Sherrell, R. M. (2008). Differential effects of phosphorus limitation on cellular metals in Chlorella and Microcystis. *Limnol. Oceanogr.* 53, 1790–1804.

Johnson, T. L., Palenik, B., and Brahamsha, B. (2011). Characterization of a functional vanadium-dependent bromoperoxidase in the marine cyanobacterium Synechococcus Sp. CC9311. *J. Phycol.* 47, 792–801.

Karl, D., Letelier, R. M., Hebel, D. V., Bird, D. F., and Winn, C.D. (1992). "Trichodesmium blooms and new nitrogen in the North Pacific gyre," in *Marine Pelagic Cyanobacteria: Trichodesmium and Other Diazotrophs*, 362nd Edn, eds E. J. Carpenter, D. G. Capone, and J. G. Rueter (Boston, MA: Kluwer Academic), 219–237.

King, A., Sañudo-Wilhelmy, S. A., Boyd, P. W., Twining, B. S., Wilhelm, S. W., Breene, C., Ellwood, M. J., and Hutchins, D. A. (2011). A comparison of biogenic iron quotas during a diatom spring bloom using multiple approaches. *Biogeosci. Discuss.* 8, 9381–9430.

Körtzinger, A., Hedges, J. I., and Quay, P. D. (2001). Redfield ratios revisited: removing the biasing effect of anthropogenic CO2. *Limnol. Oceanogr.* 46, 964–970.

Kustka, A., San Udo-Wilhelmy, S., Carpenter, E. J., Capone, D. G., and Raven, J. A. (2003a). A revised estimate of the iron use efficiency of nitrogen fixation, with special reference to the marine cyanobacterium Trichodesmium spp. (*Cyanophyta*). *J. Phycol.* 39, 12–25.

Kustka, A. B., Sañudo-Wilhelmy, S. A., Carpenter, E. J., Capone, D., Burns, J., and Sunda, W. G. (2003b). Iron requirements for dinitrogen- and ammonium-supported growth in cultures of Trichodesmium (IMS 101): Comparison with nitrogen fixation rates and iron: Carbon ratios of field populations. *Limnol. Oceanogr.* 48, 1869–1884.

LaRoche, J., and Breitbarth, E. (2005). Importance of the diazotrophs as a source of new nitrogen in the ocean. *J. Sea Res.* 53, 67–91.

Leben, R. R., Born, G. H., and Engebreth, B. R. (2002). Operational altimeter data processing for mesoscale monitoring. *Marine Geodesy* 25, 3–18.

Maldonado, M. T., and Price, N. M. (1996). Influence of N substrate on Fe requirements of marine centric diatoms. *Mar. Ecol. Prog. Ser.* 141, 161–172.

McCord, J. M., and Fridovich, I. (1969). Superoxide dismutase. *J. Biol. Chem.* 244, 6049–6055.

Mills, M. M., Ridame, C., Davey, M., La Roche, J., and Geider, R. J. (2004). Iron and phosphorus co-limit nitrogen fixation in the eastern tropical North Atlantic. *Nature* 429, 292–294.

Morel, F. M. M. (2008). The co-evolution of phytoplankton and trace element cycles in the oceans. *Geobiology* 6, 318–324.

Morel, F. M. M., and Hudson, R. J. M. (1985). "The geobiological cycle of trace elements in aquatic systems: Redfield revisited," in *Chemical Processes in Lakes*, ed. W. Stumm (New York: John Wiley), 251–281.

Núñez-Milland, D. R., Baines, S. B., Vogt, S., and Twining, B. S. (2010). Quantification of phosphorus in single cells using synchrotron X-ray fluorescence. *J. Synchrotron. Radiat.* 17, 560–566.

Orchard, E. D., Ammerman, J. W., Lomas, M. W., and Dyhrman, S. T. (2010a). Dissolved inorganic and organic phosphorus uptake in Trichodesmium and the microbial community: the importance of phosphorus ester in the Sargasso Sea. *Limnol. Oceanogr.* 55, 1390–1399.

Orchard, E. D., Benitez-Nelson, C. R., Pellechia, P. J., Lomas, M. W., and Dyhrman, S. T. (2010b). Polyphosphate in Trichodesmium from the low-phosphorus Sargasso Sea. *Limnol. Oceanogr.* 55, 2161–2169.

Orcutt, K. M., Lipschultz, F., Gundersen, K., Arimoto, R., Michaels, A. F., Knap, A. H., and Gallon, J. R. (2001). A seasonal study of the significance of N2 fixation by Trichodesmium spp. at the Bermuda Atlantic Time-series Study (BATS) site. *Deep Sea Res. Part II Top. Stud. Oceanogr.* 48, 1583–1608.

Oremland, R. S., and Stolz, J. F. (2003). The ecology of arsenic. *Science* 300, 939–944.

Payne, C. D., and Price, N. M. (1999). Effect of Cadmium toxicity on growth and elemental composition of marine phytoplankton. *J. Phycol.* 35, 293–302.

Post, A. F., Rihtman, B., and Wang, Q. (2012). Decoupling of ammonium regulation and ntcA transcription in the diazotrophic marine cyanobacterium Trichodesmium sp. IMS101. *ISME J.* 6, 629–637.

Price, N. M., and Morel, F. M. M. (1991). Colimitation of phytoplankton growth by nickel and nitrogen. *Limnol. Oceanogr.* 36, 1071–1077.

Raven, J. A. (1988). The iron and molybdenum use efficiencies of plant growth with different energy, carbon and nitrogen sources. *New Phytol.* 109, 279–287.

Redfield, A. C. (1934). "On the proportions of organic derivatives in sea water and their relation to the composition of plankton," in *James Johnstone Memorial Volume*, ed. R. J. Daniel. (Liverpool: Liverpool University Press), 176–192.

Redfield, A. C. (1958). The biological control of chemical factors in the environment. *Am. Sci.* 46, 205–221.

Redfield, A. C., Ketchum, B. H., and Richards, F. A. (1963). "The influence of organisms on the composition of seawater," in *The Sea*, ed. M. N. Hill (New York: John Wiley), 26–77.

Rubin, M., Berman-Frank, I., and Shaked, Y. (2011). Dust- and mineral-iron utilization by the marine dinitrogen-fixer Trichodesmium. *Nat. Geosci.* 4, 529–534.

Saito, M. A., Sigman, D. M., and Morel, F. M. M. (2003). The bioinorganic chemistry of the ancient ocean: the co-evolution of cyanobacterial metal requirements and biogeochemical cycles at the Archean–Proterozoic boundary? *Inorganica Chim. Acta* 356, 308–318.

Sandh, G., Xu, L., and Bergman, B. (2011). Diazocyte development in the marine diazotrophic cyanobacterium Trichodesmium. *Microbiology*. doi: 10.1099/mic.0.051268-0. [Epub ahead of print].

Sañudo-Wilhelmy, S. A., Kustka, A. B., Gobler, C. J., Hutchins, D. A., Yang, M., Lwiza, K., Burns, J., Capone, D. G., Raven, J. A., and Carpenter, E. J. (2001). Phosphorus limitation of nitrogen fixation by Trichodesmium in the central Atlantic Ocean. *Nature* 411, 66–69.

Sañudo-Wilhelmy, S. A., Tovar-Sanchez, A., Fu, F. X., Capone, D. G., Carpenter, E. J., and Hutchins, D. A. (2004). The impact of surface-adsorbed phosphorus on phytoplankton Redfield stoichiometry. *Nature* 432, 897–901.

Sheridan, C. C., Steinberg, D. K., and Kling, G. W. (2002). The microbial and metazoan community associated with colonies of Trichodesmium spp.: a quantitative survey. *J. Plankton Res.* 24, 913–922.

Sholkovitz, E. R., Sedwick, P. N., and Church, T. M. (2009). Influence of anthropogenic combustion emissions on the deposition of soluble aerosol iron to the ocean: empirical estimates for island sites in the North Atlantic. *Geochim. Cosmochim. Acta* 73, 3981–4003.

Simons, B. H., Barnett, P., Vollenbroek, E. G. M., Dekker, H. L., Muijsers, A. O., Messerschmidt, A., and Wever, R. (1995). Primary structure and characterization of the vanadium chloroperoxidase from the fungus Carvularia inaequalis. *Eur. J. Biochem.* 229, 566–574.

Sterner, R. W., and Elser, J. J. (2002). *Ecological Stoichiometry: The Biology of Elements from Molecules to the Biosphere.* Princeton, NJ: Princeton University Press.

Sunda, W. G., and Huntsman, S. A. (1995). Iron uptake and growth limitation in oceanic and coastal phytoplankton. *Mar. Chem.* 50, 189–206.

Sunda, W. G., and Huntsman, S. A. (2000). Effect of Zn, Mn, and Fe on Cd accumulation in phytoplankton: implications for oceanic Cd cycling. *Limnol. Oceanogr.* 45, 1501–1516.

Sverdrup, H. U., Johnson, M. W., and Fleming, R. H. (1942). *The Oceans, Their Physics, Chemistry, and General Biology*. New York: Prentice-Hall.

Takahashi, T., Broecker, W. S., and Langer, S. (1985). Redfield ratio based on chemical data from isopycnal surfaces. *J. Geophys. Res.* 90, 6907–6924.

Tamagnini, P., Axelsson, R., Lindberg, P., Oxelfelt, F., Wünschiers, R., and Lindblad, P. (2002). Hydrogenases and hydrogen metabolism of cyanobacteria. *Microbiol. Mol. Biol. Rev.* 66, 1–20.

Tamagnini, P., Leitão, E., Oliveira, P., Ferreira, D., Pinto, F., Harris, D. J., Heidorn, T., and Lindblad, P. (2007). Cyanobacterial hydrogenases: diversity, regulation and applications. *FEMS Microbiol. Rev.* 31, 692–720.

Tang, D., and Morel, F. (2006). Distinguishing between cellular and Fe-oxide-associated trace elements in phytoplankton. *Mar. Chem.* 98, 18–30.

Tovar-Sanchez, A., and Sañudo-Wilhelmy, S. A. (2011). Influence of the Amazon River on dissolved and intra-cellular metal concentrations in Trichodesmium colonies along the western boundary of the sub-tropical North Atlantic Ocean. *Biogeosciences* 8, 217–225.

Tovar-Sanchez, A., Sañudo-Wilhelmy, S. A., Garcia-Vargas, M., Weaver, R. S., Popels, L. C., and Hutchins, D. A. (2003). A trace metal clean reagent to remove surface-bound iron from marine phytoplankton. *Mar. Chem.* 82, 91–99.

Tovar-Sanchez, A., Sañudo-Wilhelmy, S. A., Kustka, A. B., Agustí, S., Dachs, J., Hutchins, D. A., Capone, D. G., and Duarte, C. M. (2006). Effects of dust deposition and river discharges on trace metal composition of Trichodesmium spp. in the tropical and subtropical North Atlantic Ocean. *Limnol. Oceanogr.* 51, 1755–1761.

Tuit, C., Waterbury, J., and Ravizza, G. (2004). Diel variation of molybdenum and iron in marine diazotrophic cyanobacteria. *Limnol. Oceanogr.* 49, 978–990.

Twining, B., Baines, S., Fisher, N., and Landry, M. (2004). Cellular iron contents of plankton during the Southern Ocean Iron Experiment (SOFeX). *Deep Sea Res. Part I Oceanogr. Res. Pap.* 51, 1827–1850.

Twining, B. S., Baines, S. B., Bozard, J. B., Vogt, S., Walker, E. A., and Nelson, D. M. (2011). Metal quotas of plankton in the equatorial Pacific Ocean. *Deep Sea Res. Part II Top. Stud. Oceanogr.* 58, 325–341.

Twining, B. S., Nuñez-Milland, D., Vogt, S., Johnson, R. S., and Sedwick, P. N. (2010). Variations in Synechococcus cell quotas of phosphorus, sulfur, manganese, iron, nickel, and zinc within mesoscale eddies in the Sargasso Sea. *Limnol. Oceanogr.* 55, 492–506.

Van Mooy, B. a. S., Fredricks, H. F., Pedler, B. E., Dyhrman, S. T., Karl, D. M., Koblížek, M., Lomas, M. W., Mincer, T. J., Moore, L. R., Moutin, T., Rappé, M. S., and Webb, E. A. (2009). Phytoplankton in the ocean use non-phosphorus lipids in response to phosphorus scarcity. *Nature* 458, 69–72.

Vogt, S. (2003). MAPS: A set of software tools for analysis and visualization of 3D X-ray fluorescence data sets. *Journal De Physique IV* 104, 635–638.

White, A. E., Spitz, Y. H., Karl, D. M., and Letelier, R. M. (2006). Flexible elemental stoichiometry in Trichodesmium spp. and its ecological implications. *Limnol. Oceanogr.* 51, 1777–1790.

Whittaker, S., Bidle, K. D., Kustka, A. B., and Falkowski, P. G. (2011). Quantification of nitrogenase in Trichodesmium IMS 101: implications for iron limitation of nitrogen fixation in the ocean. *Environ. Microbiol. Rep.* 3, 54–58.

Williams, R. J. P. (2001). Chemical selection of elements by cells. *Coord. Chem. Rev.* 216–217, 583–595.

Winter, J. M., and Moore, B. S. (2009). Exploring the chemistry and biology of vanadium-dependent haloperoxidases. *J. Biol. Chem.* 284, 18577–18581.

Conflict of Interest Statement: The authors declare that the research was conducted in the absence of any commercial or financial relationships that could be construed as a potential conflict of interest.

Received: 13 January 2012; accepted: 30 March 2012; published online: 26 April 2012.

*Citation: Nuester J, Vogt S, Newville M, Kustka AB and Twining BS (2012) The unique biogeochemical signature of the marine diazotroph Trichodesmium. Front. Microbio. **3**:150. doi: 10.3389/fmicb.2012.00150*

This article was submitted to Frontiers in Microbiological Chemistry, a specialty of Frontiers in Microbiology.